The effect of displacement distribution asymmetry on the accuracy of phase-shift velocimetry in porous media

Antoine Vallatos[a], Matsyendra Nath Shukla[a,b], James M. Mullin[a], Vernon R. Phoenix[a], William. M. Holmes[a]

[a] Glasgow Experimental MRI Centre, Institute of Neuroscience and Psychology, University of Glasgow, United Kingdom.

[b] School of Geographical and Earth Sciences, University of Glasgow, United Kingdom.

1 Introduction

Characterising fluid flow within porous media is of great importance for a wide range of research fields ranging from chemical engineering to geology. Accurate velocimetry can be crucial in understanding transport processes and developing models. The ability to probe flow properties in opaque systems makes MRI velocimetry based on the use of pulsed magnetic field gradients (PFG) a precious tool for the characterisation of flow in porous media. There are two main methods of PFG velocimetry, propagator velocimetry and phase-shift velocimetry. Propagator velocimetry requires several gradient encoding steps to resolve the probability distribution of displacements for each voxel. Phase-shift velocimetry is faster, requiring only two gradient encoding steps to measure the average voxel velocity.

Phase-shift velocimetry has been used to probe flow in numerous porous systems: rocks [1, 2], multiphase flow [3], fixed-bed reactors[4], microfluidic devices[5], filters [6] and bio-films [7]. However, several authors reported velocimetry inaccuracies and, despite quantitative measurement reports [2], this technique is often considered unreliable in porous media. The main issue comes from disagreements between measured and theoretical velocity values. Typically, measured values are found to be underestimated at higher flow rates [8] leading to a non-linear relationship between measured velocity and imposed flow rate [9, 10]. Additionally, velocimetry outcomes have been shown to vary with experimental parameters, such as the flow encoding gradient strength (G) [1] or the observation time (Δ) [10]. Several error causes have been proposed, including acceleration artefacts and phase contributions [11], flow related eddy current effects [9], partial-volume effects [12], velocity distribution asymmetry within the voxels [1] and relaxation effects [10].

Studying flow through sandstone rock [13], we suggested that the presence of asymmetric intra-voxel displacement distributions was the main source of these velocimetry errors. Phase-shift velocimetry relies on the assumption of symmetric intra-voxel displacements, allowing to replace displacement distributions by the average displacement [14]. But this assumption is often not valid in porous media, where asymmetric intra-voxel displacements, often related to stagnating or differential flow, are commonly encountered. A deeper and formal understanding of the effect of such

asymmetries is needed in order to achieve reliable phase-shift velocimetry. In this work, we evaluate the accuracy of phase-shift velocimetry using a phantom generating controllable displacement distributions within a single voxel. The simplicity of the set up excludes other sources of error found in the literature. Comparing measured phase values with simulated phase values based on experimental propagator data, we clearly demonstrate that important measurement errors are quantitatively related to displacement distribution asymmetries.

2 Theory

PFG NMR velocimetry consists of making the NMR signal sensitive to translational motion. First, a magnetic field gradient of amplitude G and duration δ imposes a spatially dependent phase, φ, to each nuclear spin moving along a path $\boldsymbol{r}(t)$:

$$\varphi(t) = \gamma \int_0^t \boldsymbol{G}(t) \cdot \boldsymbol{r}(t) dt \quad (1)$$

where γ is the gyromagnetic ratio. Second, after an observation time Δ, a rephasing gradient is applied. For a spin displacement $\boldsymbol{R}$, the resulting phase-shift is given by $\boldsymbol{q} \cdot \boldsymbol{R}$, with $\boldsymbol{q} = \gamma\delta\boldsymbol{G}$. The overall NMR signal resulting from a spatially resolved PFG NMR experiment can be expressed by:

$$S(\boldsymbol{k}, \boldsymbol{q}) = \iint \rho(\boldsymbol{r}) P_{\Delta}(\boldsymbol{R}, \boldsymbol{r}) e^{i\boldsymbol{k}\cdot\boldsymbol{r}} e^{i\boldsymbol{q}\cdot\boldsymbol{R}} d\boldsymbol{r} d\boldsymbol{R} \quad (2)$$

where $\rho(\boldsymbol{r})$ is the spin density and $P_{\Delta}(\boldsymbol{R}, \boldsymbol{r})$ the normalised probability distribution of displacements $\boldsymbol{R}$ during Δ, also called a propagator. For a single velocity encoding gradient direction and considering a displacement Z of each spin during Δ, the NMR signal for a voxel situated at position $\boldsymbol{r}$ is given by:

$$S(\boldsymbol{r}, q) = \rho(\boldsymbol{r}) \int P_{\Delta}(Z, \boldsymbol{r}) e^{iqZ} dZ \quad (3)$$

Defining the average velocity of each spin as $\bar{v} = Z/\Delta$, it is possible to rewrite equation 3 as:

$$S(\boldsymbol{r}, q) = \rho(\boldsymbol{r}) \int P_{\Delta}(\bar{v}, \boldsymbol{r}) e^{iq\bar{v}} d\bar{v} \quad (4)$$

If the time integral of the velocity encoding gradient is zero, this integral is independent of spin position and $S(\boldsymbol{r}, q)$ is the Fourier transform of the velocity-density function $P_{\Delta}(\bar{v}, \boldsymbol{r})$.

Propagator velocimetry consists in acquiring $S(\boldsymbol{r}, q)$ for several q values (q-steps) and then applying an inverse Fourier transform to obtain the propagator $P_{\Delta}(Z, \boldsymbol{r})$. The average velocity is given by the ratio of the average displacement ($\bar{Z}$) to the observation time Δ. The number of q-steps (typically ≥ 8) and their size has to be selected appropriately so as to cover the intra-voxel displacement range and get the desired propagator resolution.

Phase-shift velocimetry is based on a relation between velocity and the phase of the PFG NMR signal. By inserting the expression of the average voxel velocity, $V(\boldsymbol{r}) = \int \bar{v} P_{\Delta}(\bar{v}, \boldsymbol{r}) d\bar{v}$, into equation 4 one obtains:

$$S(\boldsymbol{r}, q) = \rho(\boldsymbol{r}) e^{iqV(\boldsymbol{r})\Delta} \int P_{\Delta}(\bar{v}, \boldsymbol{r}) e^{iq(\bar{v} - V(\boldsymbol{r}))\Delta} d\bar{v} \quad (5)$$

Assuming the velocity density function is symmetric around the mean velocity $\bar{v}$ then the integral in equation 5 is real and the phase of the resulting signal is found to be proportional to the average velocity:

$$\varphi(\boldsymbol{r}) = q\Delta V(\boldsymbol{r}) \quad (6)$$

In theory, one can obtain a velocity map, by subtracting two phase images obtained with different q values, using equation 7:

$$\Phi(\boldsymbol{r}) = \varphi_2(r) - \varphi_1(r) = (q_2 - q_1)\Delta V(\boldsymbol{r}) \quad (7)$$

In practice, the phase-shift effectively measured can be expressed as [14]:

$$\Phi(\boldsymbol{r}) = (q_2 - q_1)\Delta V(r) + \alpha(\boldsymbol{r}) + \theta(\boldsymbol{r}) \quad (8)$$

where $\alpha(\boldsymbol{r})$ corresponds to phase contributions that depend on q and $\theta(\boldsymbol{r})$ is phase shift caused by noise-related measurement uncertainties. By acquiring a phase-shift map at zero flow,$\Phi_0(\boldsymbol{r})$, it is possible to remove phase contributions that are not flow related:

$$\Phi(\boldsymbol{r}) - \Phi_0(\boldsymbol{r}) \simeq (q_2 - q_1)\Delta V(\boldsymbol{r}) + \theta(\boldsymbol{r}) - \theta_0(\boldsymbol{r}) \quad (9)$$

Although noise is expected to be negligible in the present work, it can become important when studying flow in porous media where the signal-to-noise ratio is not high enough to satisfy $\theta(\boldsymbol{r}) \ll (q_2 - q_1)\Delta V(\boldsymbol{r})$ [1].

3 Experimental

Experiments were performed on a horizontal 7 T Bruker Avance Biospec system (300 MHz), with a BGA12SL micro imaging gradient insert (600 mT m^{-1}) and 200-A gradient amplifiers. The birdcage Radio-Frequency volume resonator had an inner diameter of 72 mm. For flow experiments, two hard polystyrene tubes of 1 cm inner diameter and 30 cm length were used. Syringe pumps (Graseby 3100, UK) provided steady flow of a doped water solution ([$CuSO_4$] = 6.3 mM) through silicon tube connections. For generating symmetric displacement distributions a single tube was filled with water flowing at a flow rate, *Q*, of 1.2 ml min^{-1} (Figure 1a). Asymmetric distributions were achieved by filling the second tube, parallel to the first, with stationary water (Figure 1b).

3.1 MRI techniques

PFG NMR experiments were performed using an Alternating Pulsed Gradient Stimulated Echo (APGSTE) pulse sequence [13]. The 90° and 180° gauss pulses were of 1.2 ms and 2.4 ms respectively, the echo time (TE) was 5.7 ms and the repetition time (TR) was 5000 ms. Measurements were performed on a 10 mm slice along the length of the tubes. The duration of the flow encoding alternating gradients was 1ms (δ = 2 ms), the observation time, Δ, varied from 50 ms to 200 ms and the gradient varied along the direction of the flow from -25 mT m^{-1} to 25 mT m^{-1}. Experiments used 32 q values evenly distributed around q = 0 m^{-1}. Propagators, $\mathrm{P}(\Delta, Z)$, were obtained by normalisation of the inverse Fourier transform of the resulting signal against q. The phase for each q step was calculated by $\varphi = \arctan(\mathrm{S_Y}/\mathrm{S_X})$, where S_X and S_Y are respectively the real and imaginary components of the acquired complex signal [1].

3.2 Simulations of phase measurements

A MATLAB code was developed interrogate the phase behaviour using experimental propagator data [13]. Two phase types were calculated:

The average imparted phase, that corresponds to the average of individual phases imparted on the spin ensemble by the PFG gradients and is associated with phase-shift velocity mapping using equation 6. For a given q value, the phase imparted by a displacement Z_i is $\varphi_\mathrm{i} = qZ_\mathrm{i}$. Each point i in the propagator relates Z_i to its probability P_i. The total phase imparted in a voxel presenting the distribution of displacements given by an n-point propagator is therefore:

$$\varphi_{\mathrm{averagesim}} = \sum_1^n(\varphi_\mathrm{i} \times \mathrm{P_i}) = \sum_1^n(q\mathrm{Z_i} \times \mathrm{P_i}) \quad (10)$$

The simulated measured phase, that is generated from the sum of the real and imaginary components of individual spins. Here, for each gradient value, phase is calculated by:

$$\varphi_{\mathrm{measuredsim}} = \arctan\left(\frac{\sum_1^n(\cos(\varphi_\mathrm{i}+\varphi_{offset})\times \mathrm{P_i})}{\sum_1^n(\sin(\varphi_\mathrm{i}+\varphi_{offset})\times \mathrm{P_i})}\right) - \varphi_{offset} = \quad (11)$$

Where φ_{offset} is the experimental phase offset at q = 0 m^{-1}, calculated using four symmetrically distributed q-space measurements. Note that the NMR signal phase is given by the vector sum of individual spin components (measured phase) and not by the average phase of spins (average imparted phase).

4 Results and discussion

Figure 1a shows propagators measured in a large single voxel using a single flow tube set up, whereas Figure 1b shows propagators measured using one flowing and one stationary tube. In both cases, the average velocity ($V = \bar{Z}/\Delta$) is in agreement with expected values calculated using the imposed flow rate and tube radius: 0.255±0.005 mm s^{-1} for the single tube set up and 0.128±0.005 mm s^{-1} for the two tube set up. For Δ

= 50 ms, less accurate measurements were observed, with 4% difference from the theoretical velocity value, compared to less than 2% for Δ > 50 ms. This is probably due to the lower propagator resolution. The single tube flow exhibits symmetric propagators in the voxel for all observation times. The introduction of the stationary flow tube is shown to compromise the symmetry, with the effect becoming stronger as Δ increases. Note that by using same dimension parallel tubes the area under the stationary and flowing components of the asymmetric propagators are expected to be equal.

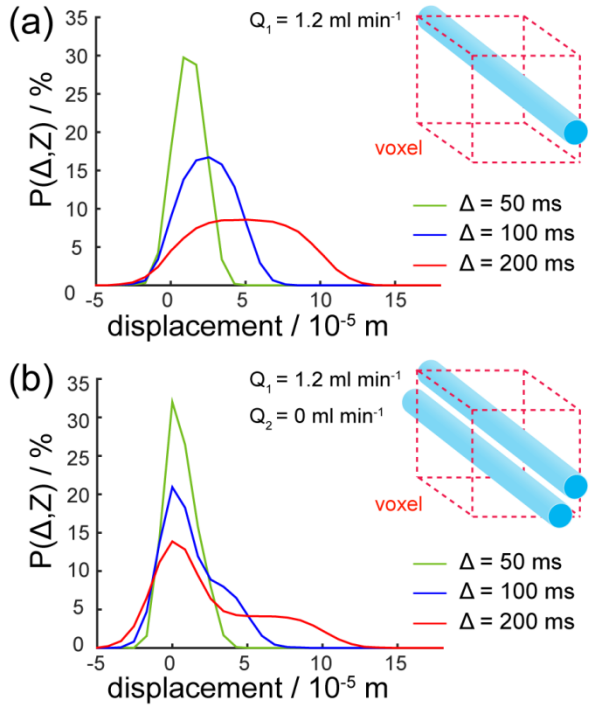

Figure 1. Probability distribution of molecular displacements (propagators) measured for the (a) symmetric and (b) asymmetric intra-voxel displacement distribution set ups.

Figure 2a,b shows the experimental phase (dots), $\varphi(q)$, acquired at the echo maximum for symmetric and asymmetric propagators. For the symmetric displacement distribution a linear $\varphi(q)$ relationship was observed, while for the asymmetric displacement distribution the linearity seems compromised, with the effect becoming stronger as Δ increases. The non-linear $\varphi(q)$ relation prevents the use of equation 6 that allows calculating average velocity using the measured phase, inevitably leading to velocimetry errors. The same effect has been reported in sandstone sample studies [1, 13], but with the present experimental set up, previously given explanations of the phenomenon do not apply: relaxation and eddy current effects are minimised by using cylindrical water tubes instead of a porous material and acceleration effects are eliminated by the use of non-pulsatile syringe pumps. Having ruled out other possible causes for the non-linearity, it is possible to focus on the effect of asymmetry in the intra-voxel displacement distribution. Overplotted to the experimental data points is $\varphi_{\mathrm{measuredsim}}(q)$ (solid line), simulated directly from the experimental propagators data shown in Figure 1. For both symmetric and asymmetric distribution cases there is very

good agreement between the simulated and the measured data, including at high observation times where $\varphi(q)$ becomes non-linear. This strongly suggests that asymmetries in intra-voxel displacement distributions are the source of $\varphi(q)$ non-linearities. Comparison between $\varphi_{\mathrm{averagesim}}$ and $\varphi_{\mathrm{measuredsim}}$ allows evaluation of the importance of the phase measurement error. While phase error is negligible (< 1%) in the symmetric distribution case (Figure 2c), important phase errors were observed in the asymmetric distribution case (Figure 2d). At higher observation times (Δ = 200 ms), where propagator asymmetries become more significant, phase errors reached 60% of the expected phase for this q range. Depending on the q values used for the velocity calculations (equation 7), this can lead to more or less important velocimetry errors.

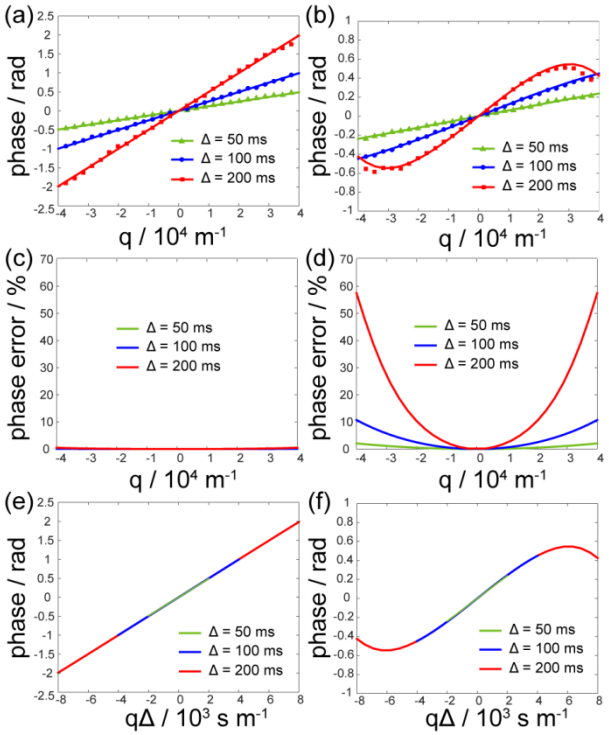

Figure 2. Measured phase against q (dots) and measurement simulation based on the propagator data shown in Figure 1 (lines) for (a) symmetric and (b) asymmetric displacement distribution set ups. Phase error calculated by $(\varphi_{averagesim} - \varphi_{measuredsim})/\varphi_{averagesim}$ *for (c) symmetric and (d) asymmetric displacement distribution. Phase measurement simulation data plotted against* $q\Delta$ *for (e) symmetric and (f) asymmetric displacement distribution.*

Increasing the flow rate (Q) is also expected to affect propagator shape, and hence $\varphi(q)$ linearity, in a similar manner to observation time. From equation 6, it is expected that $\varphi(q\Delta)$ plots give a single line for symmetric propagators (Figure 2e). Interestingly, in the case of asymmetric propagators $\varphi(q\Delta)$ plots also appear to superimpose onto the same curve (Figure 2f). It becomes clear that reducing $q \times \Delta$ allows moving towards the linear region of $\varphi(q\Delta)$ and, hence, minimise phase-shift velocimetry errors (Figure 2d). For example, using a limited number of ***q***-space values near the origin and relating velocity to the slope of the curve, Romanenko *et al.* [2] achieved accurate phase-shift

velocimetry in rocks. But this approach is often challenging in porous media since the $q \times \Delta$ reduction also reduces the imparted phase shift, which makes the measurements prone to phase noise errors that can result in noise-dominated spatial velocity distributions if the SNR is not high enough [13].

5 Conclusion

Phase-shift velocimetry has been widely used to investigate flow properties in numerous porous systems. However, several authors have reported errors in velocity measurements that were speculated upon but largely left unexplained. An often overlooked assumption in the theory of phase-shift velocimetry is that the intra-voxel displacement distributions are symmetric. This assumption, which greatly simplifies the mathematics to that shown in equation 6, is not always valid in porous media, where stagnant pores and differential flows produce asymmetric propagators. Here, we used simulations of the PFG signal, based on experimental propagator measurements, to investigate the effect of asymmetries in the propagator. The excellent agreement between experimental $\varphi(q)$ data and our simulations, strongly suggests that intra-voxel displacement distribution asymmetries are the main source of phase-shift velocimetry errors. A formal understanding of their effect could allow the development of a robust methodology for achieving more accurate velocimetry. Hence, future theoretical and experimental work will focus on relating the properties of the displacement distribution to the phase measured by PFG experiments.

Acknowledgements

This work was undertaken with financial support from the Engineering and Physical Sciences Research Council, UK (EP/J017493/).

[1] C.T.P. Chang, A.T. Watson, NMR imaging of flow velocity in porous media, AIChE J., 45 (1999) 437-444.
[2] K. Romanenko, D. Xiao, B.J. Balcom, Velocity field measurements in sedimentary rock cores by magnetization prepared 3D SPRITE, J. Magn. Reson., 223 (2012) 120-128.
[3] W.M. Holmes, K.J. Packer, Investigation of two phase flow and phase trapping by secondary imbibition within Fontainebleau sandstone, Magn. Reson. Imaging, 21 (2003) 389-391.
[4] M.D. Mantle, A.J. Sederman, L.F. Gladden, Single- and two-phase flow in fixed-bed reactors: MRI flow visualisation and lattice-Boltzmann simulations, Chem. Eng. Sci., 56 (2001) 523-529.
[5] T.Z. Teisseyre, J.L. Paulsen, V.S. Bajaj, N.W. Halpern-Manners, A. Pines, Compressive sampling with prior information in remotely detected MRI of microfluidic devices, J. Magn. Reson., 216 (2012) 13-20.
[6] F. Heese, P. Robson, L. Hall, Magnetic resonance imaging velocimetry of fluid flow in a clinical blood filter, AIChE J., 51 (2005) 2396-2401.
[7] M.A. Bernstein, K.F. King, Z.J. Zhou, Handbook of MRI pulse sequences, Academic Press, Amsterdam ; Boston, 2004.
[8] M.R. Merrill, Local Velocity and Porosity Measurements inside Casper Sandstone Using MRI, AIChE J., 40 (1994) 1262-1267.

[9] R.A. Waggoner, E. Fukushima, Velocity distribution of slow fluid flows in Bentheimer sandstone: An NMRI and propagator study, Magn. Reson. Imaging, 14 (1996) 1085-1091.
[10] N. Spindler, P. Galvosas, A. Pohlmeier, H. Vereecken, NMR velocimetry with 13-interval stimulated echo multi-slice imaging in natural porous media under low flow rates, J. Magn. Reson., 212 (2011) 216-223.
[11] R. Frayne, B.K. Rutt, Understanding Acceleration Induced Displacement Artifacts in Phase-Contrast MR Velocity-Measurements, J. Magn. Reson. Imaging, 5 (1995) 207-215.
[12] C. Tang, D.D. Blatter, D.L. Parker, Accuracy of Phase-Contrast Flow Measurements in the Presence of Partial-Volume Effects, J. Magn. Reson. Imaging, 3 (1993) 377-385.
[13] M.N. Shukla, A. Vallatos, V.R. Phoenix, W.M. Holmes, Accurate phase-shift velocimetry in rock, J. Magn. Reson., 267 (2016) 43-53.
[14] A. Caprihan, S.A. Altobelli, E. Benitezread, Flow-Velocity Imaging from Linear-Regression of Phase Images with Techniques for Reducing Eddy-Current Effects, J. Magn. Reson., 90 (1990) 71-89.

Figure Captions:

Figure 1. Probability distribution of molecular displacements (propagators) measured for the (a) symmetric and (b) asymmetric intra-voxel displacement distribution set ups.

Figure 2. Measured phase against q (dots) and measurement simulation based on the propagator data shown in Figure 1 (lines) for (a) symmetric and (b) asymmetric displacement distribution set ups. Phase error calculated by $(\varphi_{averagesim} - \varphi_{measuredsim})/\varphi_{averagesim}$ for (c) symmetric and (d) asymmetric displacement distribution. Phase measurement simulation data plotted against $q\Delta$ for (e) symmetric and (f) asymmetric displacement distribution.